Journal of Applied Electrochemistry **34**: 271–276, 2004.
© 2004 *Kluwer Academic Publishers. Printed in the Netherlands.*

Effect of N^+ ion implantation on the corrosion behaviour of Ti–6Al–7Nb and Ti–5Al–2Nb–1Ta orthopaedic alloys in Hanks solution

S. GOKUL LAKSHMI[1], S. TAMILSELVI[2], N. RAJENDRAN[2] and D. ARIVUOLI[3,*]
[1]*Crystal Growth Centre,* [2]*Department of Chemistry,* [3]*Department of Physics, Anna University, Chennai 600 025, India (*author for correspondence, e-mail: arivuoli@annauniv.edu)*

Received 3 June 2003; accepted in revised form 14 October 2003

Key words: electrochemical impedance spectroscopy, Hanks solution, plasma nitriding, titanium alloys, X-ray diffraction

Abstract

Ti–6Al–7Nb and Ti–5Al–2Nb–1Ta alloys were implanted with N^+ ions with an ion energy of 75 keV at a dose rate of 1×10^{17} and 1×10^{18} ions cm^{-2}. Open circuit potential (OCP) and potentiodynamic cyclic polarization measurements were carried out on the titanium alloys in Hanks solution to assess their corrosion resistance. The tendency for repassivation is higher in the case of implanted alloys than in untreated alloys owing to the formation of stable passive films. The impedance data showed a decrease in the double layer capacitance and an increase in the charge transfer resistance of the treated alloys. Nitrogen ion implanted Ti–6Al–7Nb was found to be more corrosion resistant than implanted Ti–5Al–2Nb–1Ta alloy.

1. Introduction

Titanium and its alloys are used in orthopaedic applications owing to their favourable mechanical properties and their excellent corrosion resistance. Among the titanium alloys, Ti–6Al–4V alloy has been widely used. It has been reported that the metal ions, particularly vanadium released into the surrounding tissues, have toxic effects [1, 2]. So vanadium free titanium alloys Ti–6Al–7Nb and Ti–5Al–2Nb–1Ta are currently used as an alternative to Ti–6Al–4V, where V is replaced by Nb which is also a β phase stabilizer. Recent studies have also discussed the long-term biocompatibility of Ta, Nb, Zr and Mo [3–5].

High corrosion resistance, excellent wear and friction resistance are desired because the properties must be similar to those of natural bone. To improve the wear resistance of titanium and its alloys, they are subjected to various surface treatments such as thermal spraying, plasma vapour deposition processes, anodic oxidation, ion implantation, glow discharge nitriding and laser treatment [6–8]. Among the above treatment methods, nitrogen ion implantation of titanium alloys has been reported to enhance the passivity and reduce the corrosion kinetics of the surface with an increasing tendency for repassivation [9, 10]. It also enhances the surface hardness and wear and friction resistance by the formation of TiN and TiC surface layers [11]. In the present study, Ti–6Al–7Nb and Ti–5Al–2Nb–1Ta alloys were nitrogen ion implanted with an acceleration voltage of 75 keV and the corrosion behaviour of the implanted alloys was studied using potentiodynamic polarization and impedance measurements.

2. Experimental details

Orthopaedic titanium alloys Ti–6Al–7Nb and Ti–5Al–2Nb–1Ta obtained from GS Titanium Inc. (US) and Kobe Steel Ltd (Japan) were used. Prior to ion implantation, the sample surfaces were mechanically polished using SiC sheets and with a 0.5 μm alumina finish to achieve a clean, smooth surface. After polishing, the specimens were decreased ultrasonically in acetone, washed with double distilled water and dried.

Nitrogen ion implantations were performed using a 200 keV ion beam generator using the Isotope Separator and Ion Implanter (ISOSIIM) at Saha Institute of Nuclear Physics, Kolkatta (India). An acceleration voltage of 75 keV and a beam current of 30 μA were employed. The alloys were implanted at a dose rate of 1×10^{17} and 1×10^{18} ions cm^{-2}. Vickers microhardness measurements were carried out using a Leitz microhardness tester at loads of 25 – 500 g. Ti_2N and Ti phases were identified by X-ray diffraction (XRD) measurements using CuK_α radiation.

The electrochemical measurements were carried out using a three electrode cell assembly with a platinum gauze counter electrode and a saturated calomel reference

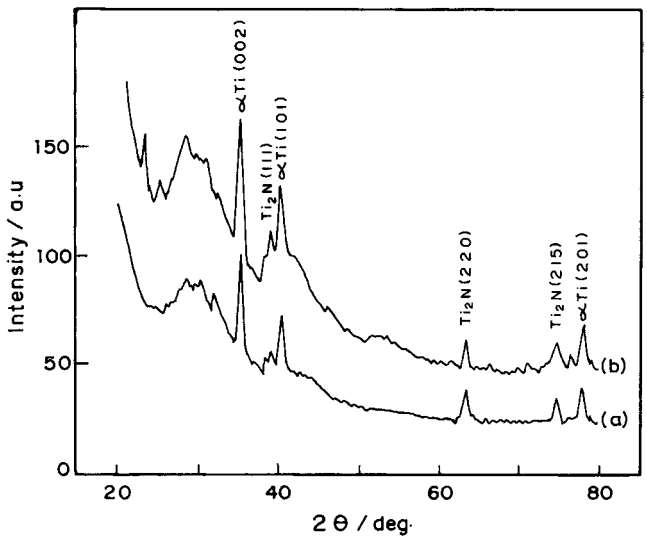

Fig. 1. X-ray diffraction pattern for Ti–6Al–7Nb alloy nitrogen implanted at dose of (a) 1×10^{17} ions cm^{-2} and (b) 1×10^{18} ions cm^{-2}.

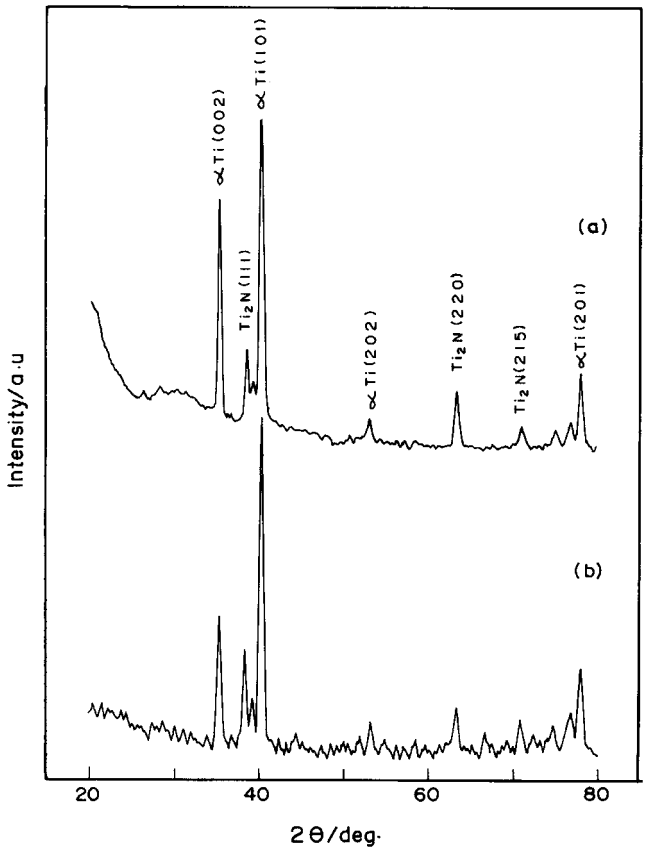

Fig. 2. X-ray diffraction pattern for Ti–5Al–2Nb–1Ta alloy nitrogen implanted at dose of (a) 1×10^{17} ions cm^{-2} and (b) 1×10^{18} ions cm^{-2}.

electrode. The specimen acted as a working electrode. The electrolyte used was a Hanks solution containing (g l^{-1}) 0.185 $CaCl_2$, 0.4 KCl, 0.06 KH_2PO_4, 0.1 $MgCl_2$ $6H_2O$, 0.1 $MgSO_4$. 7 H_2O, 8.0 NaCl, 0.35 $NaHCO_3$, 0.48 Na_2HPO_4 and 1.00 D glucose. The pH of the solution was maintained at 7.4.

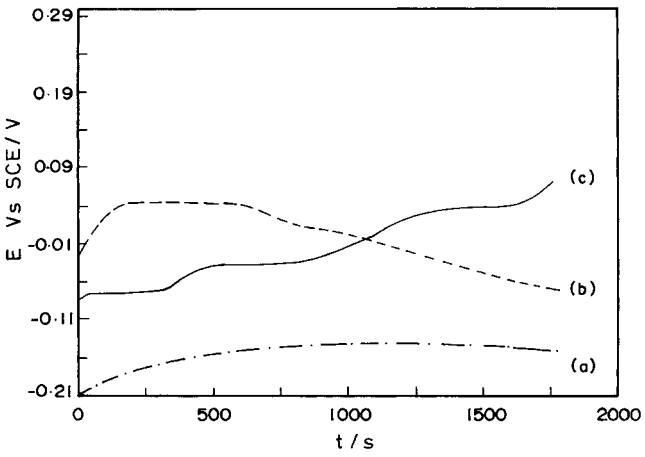

Fig. 3. OCP potential against time for (a) untreated Ti–6Al–7Nb and alloy nitrogen implanted at dose of (b) 1×10^{17} ions cm^{-2} and (c) 1×10^{18} ions cm^{-2}.

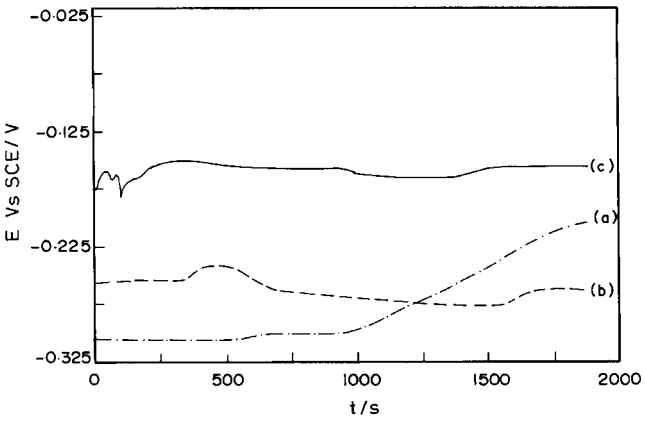

Fig. 4. OCP potential against time for (a) untreated Ti–5Al–2Nb–1Ta and alloy nitrogen implanted at dose of (b) 1×10^{17} ions cm^{-2} and (c) 1×10^{18} ions cm^{-2}.

Open circuit potential (OCP) measurements were carried out in Hanks solution for 30 min to access the corrosion behaviour under equilibrated conditions. The potentiodynamic polarization studies were conducted by immersing the working electrode in Hanks solution after 30 min. The potential was increased at a rate of 1 mV s^{-1} starting at the rest potential. Triplicate measurements were carried out in all cases. The corrosion resistance of the alloys was evaluated by measuring the difference between the breakdown potential and repassivation potential. The repassivation potential was noted as the value of potential at which the current density returned to the passive current density in the reverse scan. Generally, the smaller the difference between these values the better is the corrosion resistance.

Impedance measurements were performed by applying a sinusoidal wave of 10 mV to the working electrode in the frequency range 0.1 MHz to 10 mHz in order to measure the values of double layer capacitance and charge transfer resistance. All the tests were performed at 37 °C using an Autolab Potentiostat 12 with a frequency response analyser (FRA).

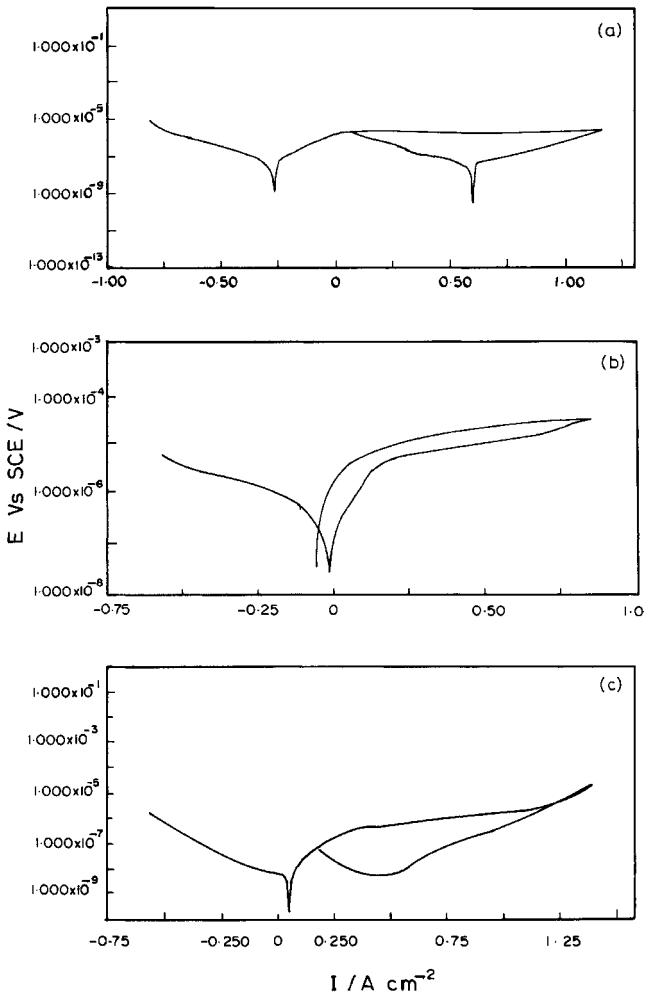

Fig. 5. Cyclic polarization curves for Ti–6Al–7Nb alloy in Hanks solution: (a) untreated, (b) 1×10^{17} ions cm^{-2} and (c) 1×10^{18} ions cm^{-2}.

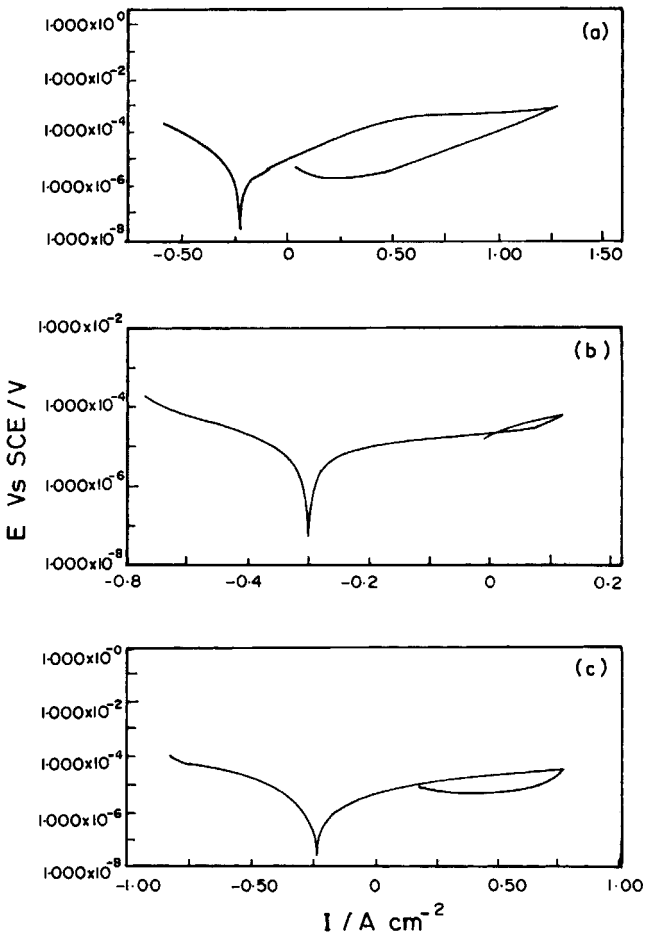

Fig. 6. Cyclic polarization curves for Ti–5Al–2Nb–1Ta alloy in Hanks solution: (a) untreated, (b) 1×10^{17} ions cm^{-2} and (c) 1×10^{18} ions cm^{-2}.

3. Results and discussion

3.1. *Phase identification*

X-ray diffraction measurements were carried out using CuK_α radiation at a scan rate of 1° min^{-1} to identify the phases formed after ion implantation. Figures 1 and 2 show the X-ray diffractogram of the N^+ implanted Ti–6Al–7Nb and Ti–5Al–2Nb–1Ta alloys at different doses. The values were compared with standard JCPDS data. Titanium nitride (Ti_2N) peaks were observed for all the implanted alloys and the peak intensity was found to increase with increase in the implanted dose.

3.2. *Electrochemical measurements*

Open circuit potentials (OCP) for untreated and N^+ ion implanted Ti–6Al–7Nb and Ti–5Al–2Nb–1Ta alloys in Hanks solution are shown in Figures 3 and 4. The OCP was found to move significantly in the noble direction for alloys implanted at a dose of 1×10^{18} ions cm^{-2} and the maximum shift in OCP was observed for the Ti–6Al–7Nb alloy when compared to Ti–5Al–2Nb–1Ta alloy. This noble shift in potential indicates the formation of a stable and protective film. Previous studies have reported similar behaviour for CP Ti, Ti–6Al–4V and Ti–6Al–7Nb alloys [12, 13].

The potentiodynamic cyclic polarization curves obtained for untreated and N^+ implanted Ti–6Al–7Nb and

Table 1. Electrochemical parameters and area of repassivation of Ti–6Al–7Nb alloy nitrogen implanted at different doses

Specifications	E_{corr} vs SCE /V	I_{corr} /A cm^{-2}	*Corrosion rate /mm a^{-1}	Area of repassivation /mm^2
Untreated	−0.265	258×10^{-8}	305×10^{-4}	320
1×10^{17} ions cm^{-2}	−0.012	2.13×10^{-8}	8.89×10^{-4}	255
1×10^{18} ions cm^{-2}	−0.081	2.74×10^{-8}	0.114×10^{-4}	243

* That is, mm per annum.

Table 2. Electrochemical parameters and area of repassivation of Ti–5Al–2Nb–1Ta alloy nitrogen implanted at different doses

Specifications	E_{corr} vs SCE /V	I_{corr} /A cm^{-2}	*Corrosion rate /mm a^{-1}	Area of repassivation /mm^2
Untreated	−0.259	2.27×10^{-7}	2.67×10^{-3}	260
1×10^{17} ions cm^{-2}	−0.302	2.52×10^{-7}	10.5×10^{-3}	170
1×10^{18} ions cm^{-2}	−0.226	1.25×10^{-7}	5.21×10^{-3}	140

* That is, mm per annum.

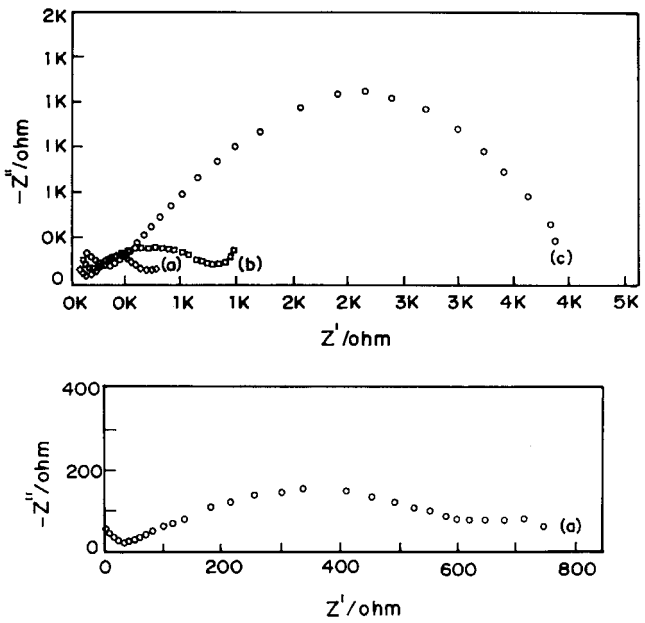

Fig. 7. Impedance diagrams obtained for Ti–6Al–7Nb alloy after immersion in Hanks solution for 96 h: (a) untreated, (b) 1×10^{17} ions cm^{-2} and (c) 1×10^{18} ions cm^{-2}.

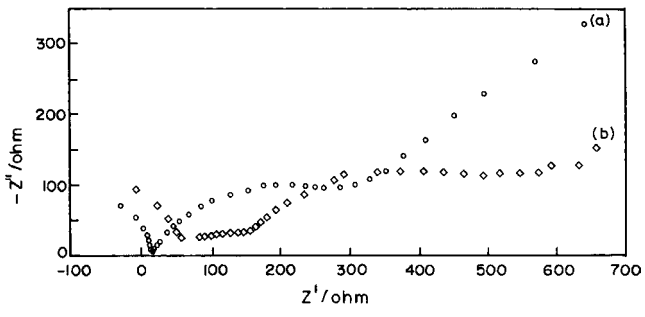

Fig. 8. Impedance diagrams obtained for Ti–5Al–2Nb–1Ta alloy after immersion in Hanks solution for 96 h: (a) untreated and (b) 1×10^{18} ions cm^{-2}.

Ti–5Al–2Nb–1Ta titanium alloys under different conditions are shown in Figures 5 and 6. In analysing the polarization curve, the corrosion potential, the critical current density and area of repassivation are the critical factors to be considered. From the polarization curves, current density, corrosion rate and area of repassivation were calculated and the values are given in Tables 1 and 2. The area of repassivation for the treated alloys showed lower values than that for untreated alloys. Among the treated alloys, that implanted at a dose rate of 1×10^{18} ions cm^{-2} shows a significant decrease in the area of repassivation, indicating the tendency for immediate repassivation, which leads to the formation of a stable surface film. The critical current densities for the untreated alloys also show very high values compared to the treated alloys. Among the treated alloys, the current density for alloy Ti–6Al–7Nb is less, indicating the formation of a stable passive layer. The formation of a stable film resists the mobility of chloride ions and other ions through the film [14]. However, the current density for the treated Ti–5Al–2Nb–1Ta alloy exhibited only a marginal decrease compared to that of the untreated alloy, which may be due to the inadequate energy of implantation.

3.3. *Electrochemical impedance measurements*

Figures 7 and 8 show electrochemical impedance diagrams (Nyquist plots) for the untreated and N^+ implanted Ti–6Al–7Nb and Ti–5Al–2Nb alloys after immersion in Hanks solution for 96 h. The impedance values at the lowest frequency of 10 mHz are presented in Table 3 and 4. The impedance values of the N^+ implanted alloy are higher than those of the untreated alloys. The double layer capacitance and charge transfer resistances were calculated from the impedance plots and the results are given in Tables 3 and 4. The charge transfer resistance is also high for the implanted alloy, which corresponds to corrosion at the metal/passive layer interface [15]. The non-implanted alloy shows the

Table 3. Impedance and capacitance values for untreated and nitrogen implanted Ti–6Al–7Nb alloy

Specifications	Z at 10 mHz	R_{ct} /ohms cm^2	C_{dl} /μF cm^{-2}
Untreated	7.47×10^2	6.92×10^2	1.022
1×10^{17} ions cm^{-2}	13.8×10^2	13.5×10^2	3.25×10^{-2}
1×10^{18} ions cm^{-2}	45.6×10^2	42.7×10^2	2.40×10^{-2}

Table 4. Impedance and capacitance values for untreated and nitrogen implanted Ti–5Al–2Nb–1Ta alloy

Specifications	Z at 10 mHz	R_{ct} /ohms cm^2	C_{dl} /μF cm^{-2}
Untreated	6.42×10^2	3.38×10^2	144.3
1×10^{18} ions cm^{-2}	6.58×10^2	9.74×10^2	107.1

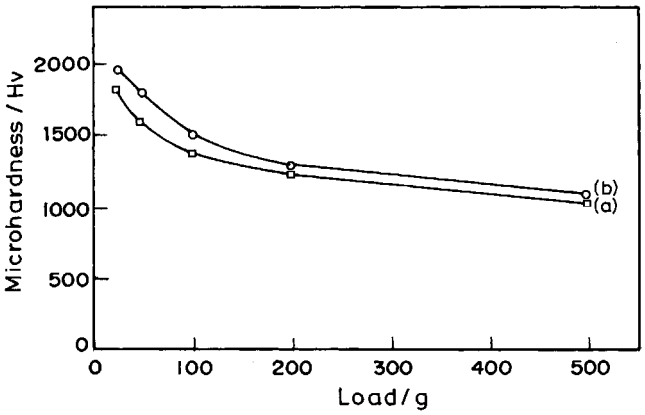

Fig. 9. Load dependant Vickers microhardness measurements for Ti–6Al–7Nb alloy: (a) 1×10^{17} ions cm^{-2} and (b) 1×10^{18} ions cm^{-2} .

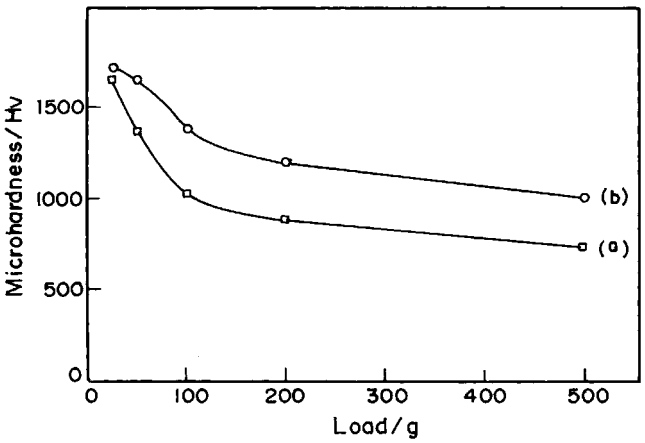

Fig. 10. Load dependant Vickers microhardness measurements for Ti–5Al–2Nb–1Ta alloy: (a) 1×10^{17} ions cm^{-2} and (b) 1×10^{18} ions cm^{-2}.

presence of diffusion elements (Figures 7(a, b) and 8), due to the formation of an interfacial film between the electrolyte and the metal. The presence of Warburg resistance was noticed for both untreated and N^+ implanted alloys, except for Ti–6Al–7Nb alloys implanted at a dose rate of 1×10^{18} ions cm^{-2}, due to the formation of an intact passive layer. Previous reports also showed that the alloys exhibit Warburg resistance indicating the presence of diffusion elements [16, 17]. This may be attributed to an insufficient ion dose and ion energy of implantation and also inadequate protection offered by the passive layer, which results in the exposure of base metal.

3.4. *Microhardness*

The Vickers microhardness was measured using a Leitz microhardness tester. Figures 9 and 10 show the load dependent microhardness of the N^+ ion implanted Ti–6Al–7Nb and Ti–5Al–2Nb–1Ta alloys at different doses. The hardness was found to decrease with increasing load. The maximum hardness obtained at 25 g load was found to be 1961 and 1714 H_v for Ti–6Al–7Nb and Ti–5Al–2Nb–1Ta alloys respectively. This is in agreement with previous work on the increase in microhardness after ion implantation for Ti–6Al–4V alloy [18].

4. Conclusions

N^+ ion implantation of Ti–6Al–7Nb and Ti–5Al–2Nb–1Ta orthopaedic alloy was conducted at an energy of 75 keV and dose of 1×10^{17} and 1×10^{18} ions cm^{-2}. Polarization and impedance measurements were carried out to evaluate the corrosion behaviour of the nitrided alloys in Hanks solution. The maximum surface hardness was found to be 1961 and 1714 H_v for Ti–6Al–7Nb and Ti–5Al–2Nb–1Ta alloys implanted at a dosage of 1×10^{18} ions cm^{-2}. The formation of Ti_2N was confirmed using XRD indicating the implantation of nitrogen ions into the surface. It was found that maximum corrosion rate and minimum area of repassivation were obtained for nitrogen ion implanted Ti–6Al–7Nb alloy. Electrochemical impedance measurements showed a decrease in the double layer capacitance value and an increase in the charge transfer resistance for the nitrogen ion implanted samples when compared to untreated specimens, indicating the formation of stable surface layer. Hence, the nitride formed on the surface by implantation acts as a barrier to the aggressive ions from the biological environment.

Acknowledgements

One of the authors S.G.L. thanks Prof. Milan Sanyal, Head of the Division of Surface Physics for providing the ion implantation facility. She is also grateful to Dr S.R. Bhattacharya, Dr T.K. Chini and other members of ISOSIIM group, SINP kolkatta, India for help with ion implantation. She also acknowledges the Council of Scientific and Industrial Research, Government of India for the award of Senior Research Fellowship and GS Titanium Inc. (US) and Kobe Steel Ltd (Japan) for providing the alloys.

References

1. J. Black, *J. Bone Joint Surg*. **70B** (1988) 517.
2. K.L. Wapner, *Clin. Orthop*. **271** (1991) 12.
3. M.F. Semlitsch, H. Weber, R.M. Streicher and R. Schon, *Biomaterials* **13** (1992) 781.
4. K. Wang, *Mater. Sci. Eng*. **A213** (1996) 134.
5. M. Niinomi, *Mater. Sci. Eng*. **A243** (1998) 231.
6. R.G. Vardiman and R.A. Kent, *J. Appl. Phys*. **53** (1982) 690.
7. J. Hongbing, L. Xia, M. Xinxin and Y. Sun, *Wear* **246** (2000) 40.
8. K.T. Rie and Th. Lampe, *Mater. Sci. Eng*. **69** (1985) 473.
9. E. Leitao, S.A. Silva and M.A. Barbosa, *Corros. Sci*. **39** (1997) 377.
10. J. Yu, Z.J. Zhao and L.X. Li, *Corros. Sci*. **35** (1993) 587.
11. S.J. Bull, P.C. Rice-Evans, A. Salei, A.J. Perry and J.R. Treglio, *Surf. Coat. Technol*. **91** (1997) 7.
12. I. Gurappa, *Mater. Character*. **49** (2002) 73.
13. L. Thair, U. Kamatchi Mudali, N. Bhuvaneswaran, K.G.M. Nair, R. Asokamani and B. Raj, *Corros. Sci*. **44** (2002) 2439.
14. M. De Becdelievre, D Fleche and J. De Becdelievre, *Electrochim. Acta* **33** (1988) 1076.
15. M. Kendig, F. Mansfeld and S. Tsai, *Corros. Sci*. **23** (1983) 317.
16. E. Chang and T.M. Lee, *Biomaterials* **23** (2002) 2917.
17. M.A. Ke, K.G. Conroy, Anna M. Fenelon, S.T. Farrell and Carmel Breslin, *Biomaterials* **22** (2001) 1531.
18. M. Li, Emile J. Knystautas and Madhavarao Krishnadev, *Surf. Coat. Technol*. **138** (2001) 220.